Journal of Biomechanics 43 (2010) 2567–2573

Contents lists available at ScienceDirect

Journal of Biomechanics

journal homepage: www.elsevier.com/locate/jbiomech
www.JBiomech.com

Effect of sulfated glycosaminoglycan digestion on the transverse permeability of medial collateral ligament

Heath B. Henninger [a], Clayton J. Underwood [a], Gerard A. Ateshian [b,c], Jeffrey A. Weiss [a,d,*]

[a] Department of Bioengineering, and Scientific Computing and Imaging Institute, University of Utah, 72S. Central Campus Drive, Salt Lake City, UT 84112, USA
[b] Department of Biomedical Engineering, Columbia University, 500 W. 120th Street, 200 S.W. Mudd, New York, NY 10027, USA
[c] Department of Mechanical Engineering, Columbia University, 500 W. 120th Street, 200 S.W. Mudd, New York, NY 10027, USA
[d] Department of Orthopedics, University of Utah, 30 North 1900 East, Rm. 3B165, Salt Lake City, UT 84132, USA

ARTICLE INFO

Article history:
Accepted 12 May 2010

Keywords:
Ligament
Permeability
Glycosaminoglycan
Chondroitinase
Stress relaxation

ABSTRACT

Dermatan and chondroitin sulfate glycosaminoglycans (GAGs) comprise over 90% of the GAG content in ligament. Studies of their mechanical contribution to soft tissues have reported conflicting results. Measuring the transient compressive response and biphasic material parameters of the tissue may elucidate the contributions of GAGs to the viscoelastic response to deformation. The hypotheses of the current study were that digestion of sulfated GAGs would decrease compressive stress and aggregate modulus while increasing the permeability of porcine medial collateral ligament (MCL). Confined compression stress relaxation experiments were carried out on porcine MCL and tissue treated with chondroitinase ABC (ChABC). Results were fit to a biphasic constitutive model to derive permeability and aggregate modulus. Bovine articular cartilage was used as a benchmark tissue to verify that the apparatus provided reliable results. GAG digestion removed up to 88% of sulfated GAGs from the ligament. Removal of sulfated GAGs increased the permeability of porcine MCL nearly 6-fold versus control tissues. Peak stress decreased significantly. Bovine articular cartilage exhibited the typical reduction of GAG content and resultant decreases in stress and modulus and increases in permeability with ChABC digestion. Given the relatively small amount of GAG in ligament ($<1\%$ of tissue dry weight) and the significant change in peak stress and permeability upon removal of GAGs, sulfated GAGs may play a significant role in maintaining the apposition of collagen fibrils in the transverse direction, thus supporting dynamic compressive loads experienced by the ligament during complex joint motion.

1. Introduction

Ligament is viscoelastic, exhibiting stress relaxation, creep, hysteresis and sensitivity to strain level and rate (Bonifasi-Lista et al., 2005; Lujan et al., 2009; Weiss et al., 2002). These characteristics may mitigate injury and failure of the tissue by dissipating energy during deformation. Understanding the structure–function relationship of constituents in ligament can elucidate the origins of the viscoelastic response. This knowledge is critical to develop microstructurally motivated constitutive models, and to understand changes in material behavior due to injury or disease, which may ultimately be useful in tissue failure analysis and designing engineered tissue replacements.

The origins of viscoelasticity in ligament are the subject of ongoing debate, but constituents of the tissue provide clues to possible sources. Ligaments contain approximately 70% Type I collagen by dry weight (Amiel et al., 1990, 1984). The wet weight of ligaments is up to 70% water and the balance of the hydrated matrix is a mixture of cells, structural proteins, proteoglycans (PGs) and their associated glycosaminoglycans (GAGs). These components and their organization may contribute to the viscoelastic response of the tissue through intrinsic solid-phase viscoelasticity, contributions from fluid movement during deformation or a combination of the two.

Sulfated GAGs have been scrutinized for their contributions to ligament and tendon viscoelasticity. GAGs and PGs constitute 0.2–5.0% of the dry weight of ligaments (Amiel et al., 1990; Gillard et al., 1977). Chondroitin-4- and 6-sulfates (CS) and dermatan sulfate (DS) constitute $>90\%$ of the sulfated GAG content in ligament (Campbell et al., 1996; Ilic et al., 2005; Vogel et al., 1993). DS and CS are typically bound to core proteins to form decorin and biglycan PGs (Iozzo, 1999). These GAGs are highly electronegative and contribute to tissue hydration (Ernst et al., 1995; Iozzo, 1998).

Enzymatic digestion of GAGs in ligament had no effect on the quasi-static or viscoelastic response of ligament under shear or tensile loading (Lujan et al., 2009, 2007). Similar results were

* Corresponding author at: Department of Bioengineering, University of Utah, 50 South Central Campus Dr., Room 2480, Salt Lake City, UT 84112, USA.
Tel.: +1 801 587 7833; fax: +1 801 585 5361.
E-mail address: jeff.weiss@utah.edu (J.A. Weiss).

0021-9290/$ - see front matter © 2010 Elsevier Ltd. All rights reserved.
doi:10.1016/j.jbiomech.2010.05.012

reported for tendon (Fessel and Snedeker, 2009; Rigozzi et al., 2009; Screen et al., 2005). These results are contrary to a proposed role of GAGs in directly transmitting forces between collagen fibrils (Redaelli et al., 2003; Scott, 2003; Seog et al., 2005). They also contrast developmental contributions of GAGs and PGs to connective tissue mechanics where their primary mechanism is regulation of collagen organization and spacing (Danielson et al., 1997; Elliott et al., 2003; Robinson et al., 2005).

Alternatively, GAGs may inhibit transient water movement (Hascall, 1977; Quinn et al., 2001; Swartz and Fleury, 2007). GAG content is a primary determinant of the compressive viscoelastic response of articular cartilage (Basalo et al., 2004; Katta et al., 2008; Korhonen et al., 2003; Maroudas and Schneiderman, 1987). GAG digestion increases permeability and decreases compressive modulus as a result of higher water mobility during deformation (Katta et al., 2008; Korhonen et al., 2003). GAG digestion also decreases interstitial fluid load support in cartilage (Basalo et al., 2004). GAGs in articular cartilage are primarily associated with the proteoglycan aggrecan, whereas ligaments and tendons are dominated by decorin and biglycan PGs. Aggrecan contains hundreds of GAG chains, but decorin and biglycan have only one or two GAG chains, respectively. Further, there is a much smaller percentage of GAGs in ligament and tendon than in articular cartilage.

Ligament may experience similar effects in compression transverse to the collagen axis. Because of their large Poisson's ratios (0.8–3.0; Hewitt et al., 2001; Lynch et al., 2003; Yin and Elliott, 2004), tensile loading results in a positive pressure gradient out of the tissue. If GAG digestion in ligament increased permeability, this would suggest decorin and biglycan GAGs modulate fluid flow-dependent viscoelasticity by limiting water movement during deformation. A decrease in peak stress after GAG digestion would indicate that GAGs maintain dynamic fluid pressurization to stiffen the tissue during deformation. A decrease in equilibrium compressive stress and modulus would demonstrate that GAGs resist static compressive loads.

Therefore, the hypotheses of this study were that enzymatic digestion of CS and DS GAGs would influence the transient compressive response of ligament, transverse to the collagen axis, as follows: peak stress, equilibrium stress and aggregate modulus would decrease, and intrinsic permeability would increase. To test the hypotheses, confined compression stress relaxation experiments were performed on control tissues and those treated to digest CS and DS GAGs.

2. Methods

2.1. Tissue isolation

Six porcine knees (age 5–8 months, mixed sex) were obtained (Frontier Biomedical). Knees were frozen at −20 °C until testing. Knees were thawed and then dissected free of extraneous soft tissue. The MCL was removed at the insertions and fine dissected to remove overlying fascia, while hydrated with Ringer's solution during isolation. MCLs were frozen to −70 °C and three neighboring samples were removed from the mid-substance using a 5 mm coring punch. The punch axis was oriented normal to the lateral anatomical surface of the ligament. This produced plugs with the predominant collagen fibers oriented normal to the test axis, i.e. the transverse plane.

Specimen thickness was measured three times with a micrometer (Model CD-6″CSX, Mitutoyo) and three times on a resistive circuit (Weiss and Maakestad, 2006). Measurements were taken at the center and opposing edges of the samples. All measurements were averaged to produce the final thickness. The average coefficient of variation (CV) in thickness measurement was 3.8% for control and 4.7% for treated tissues.

Cartilage served as a benchmark tissue to verify that the test system provided reliable results. Five skeletally mature bovine knees were obtained and three plugs of articular cartilage were removed from each lateral femoral condyle. Cartilage samples underwent the same preparation, treatments and testing as MCL samples, with the exception that full thickness cartilage was sectioned with a microtome to ensure superficial and cut surfaces were parallel.

2.2. Glycosaminoglycan digestion

Digestion with chondroitinase ABC (ChABC, Sigma) was performed on one of the three samples from each knee. ChABC degrades CS and DS and some hyaluronic acid GAGs (Ernst et al., 1995). Another sample was used as a buffer soaked control and the remaining sample was used as the native tissue control for biochemical analysis.

ChABC treatment was adapted from previous studies (Henninger et al., 2007; Lujan et al., 2007). Control buffer consisted of non-lactated Ringer's solution containing 20 mM Tris (pH 7.5) and protease inhibitors (Mini-Complete, Roche). Treatment buffer was the same as the control buffer with the addition of 1 U/ml ChABC. Excluding native samples, all samples were equilibrated for 1 h in control buffer at room temperature. Samples were then treated for an additional 6 h with either control or ChABC buffer. Wet weights were recorded at isolation and after buffer soaks. Samples were lyophilized after testing and dry weights were collected.

2.3. Glycosaminoglycan quantification and ChABC efficacy

GAG content of tissue extracts was quantified using the 1–9 dimethylmethylene blue assay (Farndale et al., 1986; Lujan et al., 2007). Absorbance was measured on a plate reader (Synergy HT, Bio-TEK) and compared to a standard curve generated from known concentrations of sulfated GAGs. Additional extract was treated overnight with ChABC to determine if additional GAG was degraded once freed from the tissue macrostructure, quantifying the efficiency of initial treatment. GAG content was normalized to tissue dry weight.

2.4. Confined compression stress relaxation

The stress relaxation protocol was adapted from (Ateshian et al., 1997). The apparatus consisted of a servo-controlled mechanical stage (Model MRV22, Tol-O-Matic, accuracy ± 1.0 μm), LVDT (Model ATA 2001, Schaevitz, accuracy ± 0.05% FS), and a 5 mm diameter confining chamber. Porous sintered stainless steel filters (Model PXX, 20 μm pores, permeability $\sim 10^{-11}$ m^4/N s, Small Parts Inc.) retained the sample within the chamber.

Samples were loaded with the primary collagen fibers transverse to the test axis. The chamber was submersed in control buffer during testing. A 20% compressive strain was applied for 1 min to seat the tissue. The actuator was then retracted to its reference position and the tissue was allowed to recover for 15 min.

An incremental tare strain (1% steps) was applied until a minute load (< 0.01 N) was detected. This ensured that the actuator was in contact with the upper filter and established the reference thickness. Tare strain (vs. tare load) was used because pilot testing indicated that ChABC treatment softened the tissue. Five incremental step displacements of 5% each (to 25% strain) were applied at 0.01%/s, each followed by 1400 s of relaxation at static displacement. A 1000 g load cell (Model 31, Sensotec, accuracy ± 0.25% FS) was used. For direct comparison to published data (Ateshian et al., 1997), a 10% strain increment (to 50% strain), was used for articular cartilage samples.

Experimental data for equilibrium Cauchy stress (σ^e) and stretch (λ) along the test axis were fit to a constitutive model for the solid phase of the material. The three-dimensional form of the model was based on the research of Cohen et al. (1998), and was used previously to determine the strain-dependent permeability of articular cartilage under confined compression (Ateshian et al., 1997; Holmes and Mow, 1990). For confined compression, strain occurs only along the test axis, and the constitutive model reduces to one-dimensional form:

$$\sigma^e = \frac{1}{2} H_a \left(\frac{\lambda^2 - 1}{\lambda^{2\beta+1}} \right) e^{(\beta(\lambda^2-1))} \tag{1}$$

Here, H_a is the aggregate modulus and β is a coefficient controlling nonlinearity. Using the experimental data for σ^e and λ and the Levenberg–Marquart method, H_a and β were determined.

H_a and β were then used in a second curve fit to determine the intrinsic permeability (k_0) and nonlinearity coefficient (M) from the following constitutive model (Holmes, 1986):

$$k = k_0 \left[\frac{J - \varphi_0}{1 - \varphi_0} \right]^2 e^{((MJ^2-1))/2)} \tag{2}$$

where k is the strain-dependent permeability, J is the volume ratio ($J = \lambda$ for confined compression) and φ_0 is the solid volume fraction. Solid fraction was determined by linearly interpolating water content after the application of tare strain between the native and free-swelling thicknesses and water contents of each sample (sample specific range: 0.22–0.28). Intrinsic permeability (k_0) is the permeability in the absence of deformation, i.e. $J = \lambda = 1$.

The finite-difference method was used to discretize the system of ordinary differential equations from the biphasic equations of motion for confined compression stress relaxation (Ateshian et al., 1997). The nonlinear system of equations was solved at each timestep using Newton's method to yield the stress–time profile. Optimized values of k_0 and M were determined by minimizing the difference between predicted and experimental stress–time profiles using a nonlinear least square method.

2.5. Statistical analysis

A pilot study showed neighboring samples provided repeatable measures of intrinsic permeability (22% CV). Differences in thickness, water and GAG content, stress, modulus and permeability between groups were analyzed using the Wilcoxon signed ranks test. Spearman's ρ tested the relationship of GAG content and intrinsic permeability. Significance was set at $p \leq 0.05$. Data are presented as mean $\pm$ SD unless noted.

3. Results

3.1. GAG quantification and efficacy of ChABC

MCL thickness (after tare strain) averaged 2.01 ± 0.19 mm for control and 2.12 ± 0.28 mm for ChABC treated tissues ($p=0.463$). Water content was $67.0 \pm 2.7\%$ for native samples, and increased with control and ChABC treatment to $78.6 \pm 1.6\%$ (from $70.8 \pm 1.8\%$) and $77.8 \pm 2.1\%$ (from $71.2 \pm 2.6\%$). Control and ChABC groups had significantly higher water content than native tissue (both $p=0.028$) but did not significantly differ themselves ($p=0.463$).

Total sulfated GAG content was 7.07 ± 1.64 μg/mg tissue dry weight for native and 8.14 ± 1.39 μg/mg for control MCL (Fig. 1) and after ChABC treatment was 1.00 ± 0.11 μg/mg (~88% reduction). There was no significant difference between native and control groups ($p=0.116$), but both were significantly higher than the ChABC group (both $p=0.028$). ChABC treated extracts digested with additional ChABC reduced sulfated GAG content to 0.95 ± 0.11 μg/mg. This represented a 5% drop in GAG content by secondary digestion, yielding 95% efficiency for the initial digestion.

3.2. Influence of ChABC on the compressive response of porcine MCL

Fig. 2 shows a representative curve fit of experimental stress–time data (top), average stress–time responses (middle), and average stress–stretch data (bottom). Coefficients of determination for control and ChABC equilibrium stress–stretch responses were $R^2=0.997 \pm 0.002$ (root-mean-squared-error [RMSE]$=0.002 \pm 0.001$ MPa) and 0.996 ± 0.002 (RMSE$=0.002 \pm 0.002$ MPa). Peak stress decreased significantly upon ChABC treatment for 5–20% strain (all $p \leq 0.043$) but did not at the 25% strain level ($p=0.138$). Equilibrium

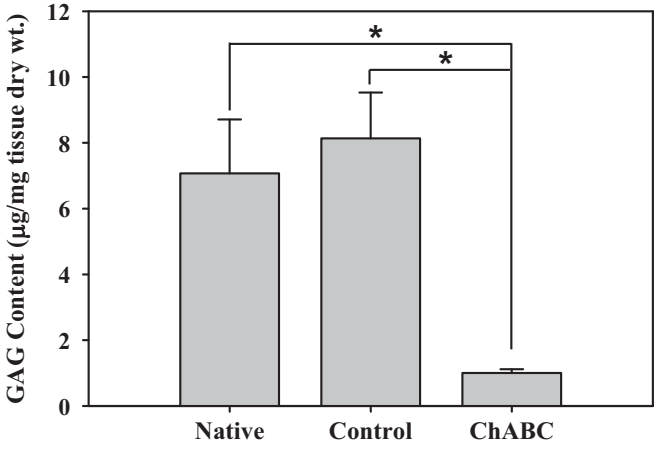

Fig. 1. Sulfated GAG content of porcine MCL normalized to tissue dry weight. ChABC treatment significantly reduced sulfated GAG content (*) as compared to native and control tissue samples. There were no statistical differences between native and control (buffer soaked) samples. GAGs remaining after digestion were likely keratin or heparin sulfates, which are not affected by ChABC (mean $\pm$ SD).

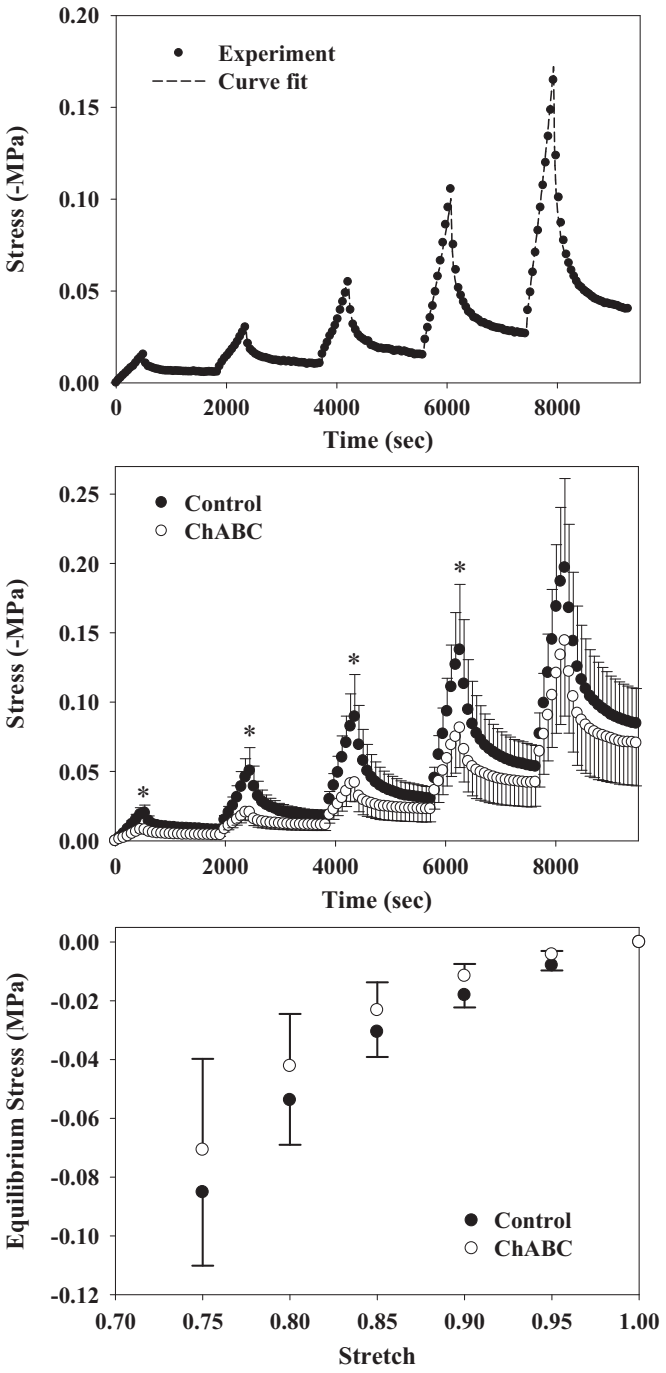

Fig. 2. Experimental data from stress relaxation testing of control and ChABC treated porcine MCL. Top: Curve fit of representative experimental ChABC stress–time data to the biphasic constitutive model for incremental stress relaxation testing. Parameters: $H_a=0.07$ MPa, $\beta=4.54$ (unitless), $k_0=15.0 \times 10^{-15}$ m^4/N s, $M=11.92$ (unitless). Middle: Average control and ChABC treated stress–time curves for the sample population ($n=6$, mean $\pm$ SEM). Peak stress dropped significantly for all but the 25% strain level (*). Bottom: Average stress–stretch curves for the sample population ($n=6$, mean $\pm$ SEM). ChABC treated samples consistently had lower stress than their control counterparts within the same knee, but there was large variance between pairs from different knees.

stress did not vary significantly at any strain level tested (all $p \geq 0.116$).

Permeability increased significantly following ChABC treatment ($p=0.028$, Fig. 3, Table 1). The aggregate modulus (H_a) was lower for ChABC treated tissues, although no significant differences were detected ($p=0.345$). Conversely, M was higher for ChABC tissues but no significant differences were detected ($p=0.249$). There was no effect of treatment on β ($p=0.249$). GAG content was negatively correlated to permeability ($\rho=-0.741$, $p=0.003$).

3.3. Verification of testing procedures with bovine articular cartilage

Cartilage thickness averaged 1.40 ± 0.31 and 1.20 ± 0.20 mm for control and ChABC treated tissues. Water content for native tissue was $81.9 \pm 3.2\%$, while control and ChABC tissues averaged $81.5 \pm 4.1\%$ and $82.9 \pm 2.5\%$. No significant differences were detected between groups for thickness ($p=0.091$) or water content (all $p \geq 0.249$). Sulfated GAG content was 212.0 ± 41.9 μg/mg dry weight for native and 201.7 ± 44.1 μg/mg for control cartilage. ChABC treatment reduced sulfated GAG content to 71.1 ± 32.6 μg/mg. Sulfated GAG content did not vary between native and control ($p=0.866$) but both were significantly higher than the tissue treated with ChABC (both $p=0.018$).

Peak and equilibrium stress decreased significantly upon ChABC treatment for all strain levels tested (10–50%, all $p=0.028$). The permeability of cartilage in the ChABC treated group was significantly higher than the control group ($p=0.018$, Fig. 3, Table 2). Aggregate modulus dropped significantly upon ChABC treatment ($p=0.028$). Coefficients of determination for control and ChABC equilibrium stress–stretch responses were $R^2=0.995 \pm 0.003$ (RMSE 0.004 ± 0.003 MPa) and 0.998 ± 0.001 (RMSE 0.001 ± 0.001 MPa), respectively. GAG content was negatively correlated to permeability ($\rho=-0.644$, $p=0.006$).

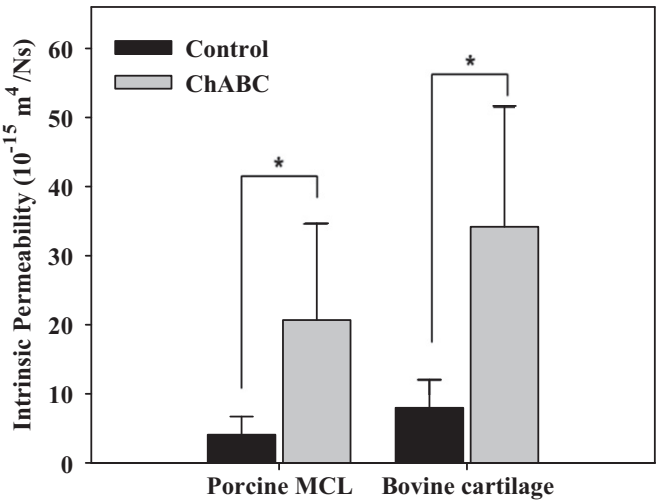

Fig. 3. Influence of CS and DS GAGs on the permeability of porcine MCL and bovine articular cartilage. Both bovine cartilage and porcine MCL showed significant increases (*) in permeability with ChABC treatment. No significant differences in permeability were detected between tissues by treatment case. Permeability of bovine cartilage was similar to previous reports (Table 2) (mean ± SD).

4. Discussion

Two of the four hypotheses of this study were confirmed. ChABC digestion caused a significant decrease in peak stress during confined compression stress relaxation (except at 25% strain) and a significant increase in transverse permeability. Equilibrium stress and aggregate modulus decreased after ChABC treatment, but the changes were not significant. Similar results were found for articular cartilage, with the exception that GAGs had a significant impact on the equilibrium compressive properties of cartilage, and these results parallel findings in the literature (Katta et al., 2008; Korhonen et al., 2002).

The results demonstrate GAGs in ligament strongly influence the transient compressive response in the transverse direction in ligament, since the reduction in GAG content from 0.8% to 0.1% induced significant changes in peak stress and permeability (Table 1, Fig. 2). GAG content was in agreement with previous reports that DS and CS were the predominant GAGs in ligament (Campbell et al., 1996; Henninger et al., 2009; Ilic et al., 2005; Lujan et al., 2009; Vogel et al., 1993). Changes in peak stress and permeability were therefore a direct result of GAG digestion, as there were no differences in other biochemical or experimental factors.

GAG content in ligaments can be up to 5.0% of dry weight (Amiel et al., 1990; Gillard et al., 1977). Changes detected in the present study might be greater for ligaments with higher GAG content. This is supported by the large impact of sulfated GAGs on all mechanical properties for articular cartilage (Basalo et al., 2004; Katta et al., 2008; Korhonen et al., 2003) since cartilage had nearly 25 times higher GAG content than the ligament.

Prior studies examining the impact of GAGs on ligament and tendon mechanics focused on tensile and shear properties (Fessel and Snedeker, 2009; Lujan et al., 2009, 2007; Rigozzi et al., 2009; Screen et al., 2005). Ligaments primarily resist tensile forces, but also experience transverse compressive strains in areas where they wrap over bone (Li et al., 2002; Sakane et al., 1999; Vogel et al., 1993). The present experiments directly quantified the influence of GAGs on the transverse compressive response of the tissue, which has not previously been reported.

Ligaments and tendons undergo significant lateral contraction during axial tensile loading (Poisson's ratio=0.8–3.0; (Hewitt et al., 2001; Lynch et al., 2003; Yin and Elliott, 2004)). This volume loss may result from the microstructural organization of the

Table 1
Comparison of material parameters from confined compression stress relaxation of porcine MCL (control vs. ChABC). Data reported as mean ± SD. Note the trend toward decreasing aggregate modulus with ChABC treatment was not significant, but could indicate softening upon digestion of sulfated GAGs. Similarly, ChABC treatment resulted in an increase in permeability.

Control/ChABC	H_a (MPa)	β (unitless)	k_0 (10^{-15} m^4/N s)	M (unitless)
Present study	$0.16 \pm 0.10/0.11 \pm 0.10$	$4.19 \pm 2.43/5.02 \pm 1.23$	$4.08 \pm 2.62/20.67 \pm 14.02$ [a]	$7.43 \pm 1.12/10.16 \pm 4.51$
Atkinson et al. (1997)	–	–	0.1–10/NA [b]	–
Adeeb et al. (2004)	–	–	10.0/NA [b]	–
van Driel et al. (2000)	–	–	10.0/NA [b]	–
Weiss and Maakestad (2006)	–	–	2.94/NA	7.98/NA

[a] Significant change between control and ChABC at $p<0.05$.
[b] Properties utilized in mechanical models of ligament.

Table 2
Comparison of material parameters from confined compression stress relaxation of full thickness articular cartilage (control vs. ChABC). Data reported as mean ± SD. Note the decrease in moduli (aggregate and Young's) and increase in permeability with ChABC treatment.

Control/ChABC	H_a (MPa)	β (unitless)	k_0 (10^{-15} m^4/N s)	M (unitless)
Present study	0.15 ± 0.10/0.03 ± 0.02 [a]	0.61 ± 0.19/0.97 ± 0.47	7.58 ± 4.31/33.9 ± 22.2 [a]	3.90 ± 0.40/6.09 ± 1.51 [a]
Ateshian et al. (1997)	0.40 ± 0.14/NA	0.35 ± 0.29/NA	2.7 ± 1.5/NA	2.2 ± 1.0/NA
Chen et al. (2001)	0.47 ± 0.11/NA	–	7.3 ± 1.73/NA	8.41 ± 1.72/NA
Katta et al. (2008)	0.44/0.27 [b]	–	0.58/1.28	–
Korhonen et al. (2003)	0.34 ± 0.04/0.12 ± 0.08 [a,b]	–	0.71 ± 0.11/1.13 ± 0.36 [a]	–
Williamson et al. (2001)	0.31 ± 0.03/NA	–	~15 ± 1/NA	~16 ± 2/NA

[a] Significant change between control and ChABC at $p < 0.05$.
[b] Young's modulus (MPa).

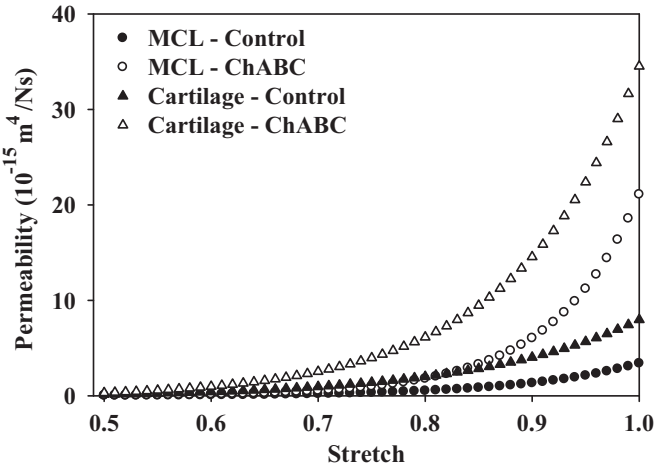

Fig. 4. Permeability as a function of applied volumetric strain (J). Since the raw data from stress relaxation testing do not provide the strain-dependent permeability directly, the intrinsic permeability (k_0) and strain-dependence parameter (M) were input to the constitutive model (Eq. (2)) and plotted over a range of compressive stretch (λ). Permeability decreased with increasing compressive strain, but curves for ChABC treated tissues decreased more rapidly than those for the control tissues. Permeability was reduced to nearly zero for all treatment groups by 50% compressive strain ($\lambda = 0.5$).

tissue (Reese et al., 2010), which could cause water exudation under tensile loading (Han et al., 2000; Wellen et al., 2004). Since GAGs are found between fibrils in ligament and tendon (Cribb and Scott, 1995; Henninger et al., 2009), their association with water likely helps resist this deformation. Experiments directly measuring Poisson's ratio as a function of GAG digestion could provide further evidence of this interaction.

The results of this study demonstrated that GAG degradation allowed more rapid water exudation (i.e. increased permeability) and reduced support of dynamic compressive loading (i.e. decreased peak stress). Therefore, when ligament experiences dynamic transverse compressive loading, interstitial fluid pressurization may contribute significantly to the tissue's dynamic compressive modulus (Basalo et al., 2004; Soltz and Ateshian, 2000). Due to the dependence of permeability on strain, this mechanism would be greatest at low volumetric strain (Fig. 4). Tissue compaction reduces porosity of the solid matrix and therefore, permeability. It is apparent that GAG digestion profoundly increases the low strain permeability. Both control and GAG depleted tissues converge to the same permeability after large compressive deformations. This may be why there was not a significant decrease in peak stress at the highest (25%) compressive strain level, highlighting the importance of GAGs in low-strain compressive support.

Removal of sulfated GAGs provided no change in β for MCL or cartilage but did affect M in cartilage. This demonstrates that GAG removal does not affect the nonlinearity of the equilibrium stress–strain response, but the magnitude may change since the matrix cannot support as much load once GAGs are removed. The change in the strain-dependence of the permeability (M) is more dramatic in cartilage once GAGs are removed, and this again may be a function of the relative quantities of GAG in the tissues.

Although there are no previous results for confined compression stress relaxation of ligament, they are considered reliable based on the results for articular cartilage in this study. Cartilage exhibited an increase in permeability after digestion of GAGs and material parameters were in good agreement with previous reports (Table 2) (Ateshian et al., 1997; Chen et al., 2001; Katta et al., 2008; Korhonen et al., 2003; Williamson et al., 2001). Sulfated GAG content in cartilage was also in agreement with the previous studies (Basalo et al., 2006; Katta et al., 2008).

Our previous study examined permeability of human MCL with direct permeation/ultrafiltration (Weiss and Maakestad, 2006) and control ligaments in the present study were in good agreement (Table 1). Other studies utilizing permeability in modeling of ligament required values similar to those presented herein (Table 1) (Adeeb et al., 2004; Atkinson et al., 1997; van Driel et al., 2000). The present study provides much needed inputs for biphasic constitutive models and is the first report of the influence of sulfated GAGs on the compressive response and permeability of ligament transverse to the collagen fibers.

Due to the anisotropy of ligaments, it is possible that the permeability of MCL along the primary fiber direction is different than transverse to the fiber direction (Federico and Herzog, 2008; Gu et al., 1999; Lynch et al., 2003; Yin and Elliott, 2004). Magnetic resonance imaging of tendon suggested that axial water diffusion was much faster than diffusion transverse to the fiber axis (Han et al., 2000; Helmer et al., 2004). Since GAGs are located in the interfibrillar space in MCL (Henninger et al., 2009), GAG removal would likely increase the permeability along the fibers even more than in the transverse direction. Given higher axial permeability, transverse deformation could pressurize tissue along the axis of collagen between bony insertions and dynamically stiffen ligament along its length.

The constitutive assumption of isotropy for the solid phase of the tissue invoked for parameter estimation is worthy of discussion. Eq. (1) was formulated for isotropic materials, but it is known that ligament and tendon are often characterized as transversely isotropic with respect to the collagen fiber direction (Gardiner and Weiss, 2003; Reese et al., 2010; Weiss et al., 2002). Inclusion of the transversely isotropic symmetry in the constitutive model would not affect the results for the present study, since testing was performed transverse to the collagen fiber direction. The combination of uniform axial compression and radial confinement during confined compression testing prevents any

strain in the transverse plane, along the collagen fiber direction, at the continuum level. It is possible that inhomogeneous deformation could have occurred at lower hierarchical levels, since fiber crimp and collagen interweaving are present at scales below the continuum level (Franchi et al., 2008; Provenzano and Vanderby, 2006). This limitation is present in any study of continuum level material properties where microstructural organization is not truly homogeneous, like the changing collagen organization through the thickness of articular cartilage (Chen et al., 2001; Huang et al., 2005; Setton et al., 1993).

In conclusion, this study has demonstrated that the sulfated GAGs in MCL modulate the transverse permeability of the tissue and thus the internal pressurization and dynamic compressive modulus during dynamic compressive deformation in the transverse direction.

Conflict of interest statement

The authors do not have any financial and personal relationships with other people or organisations that could inappropriately influence (bias) the work.

Acknowledgement

Financial support from NIH #AR47369 is gratefully acknowledged.

References

Adeeb, S., Ali, A., Shrive, N., Frank, C., Smith, D., 2004. Modelling the behaviour of ligaments: a technical note. Comput. Methods Biomech. Biomed. Eng. 7, 33–42.

Amiel, D., Billings, E., Akeson, W., 1990. Ligament structure, chemistry, and physiology. In: Daniel, D. (Ed.), Knee Ligaments Structure, Function, Injury, and Repair. Raven Press, New York, pp. 77–91.

Amiel, D., Frank, C., Harwood, F., Fronek, J., Akeson, W., 1984. Tendons and ligaments: a morphological and biochemical comparison. J. Orthop. Res. 1, 257–265.

Ateshian, G.A., Warden, W.H., Kim, J.J., Grelsamer, R.P., Mow, V.C., 1997. Finite deformation biphasic material properties of bovine articular cartilage from confined compression experiments. J. Biomech. 30, 1157–1164.

Atkinson, T.S., Haut, R.C., Altiero, N.J., 1997. A poroelastic model that predicts some phenomenological responses of ligaments and tendons. J. Biomech. Eng. 119, 400–405.

Basalo, I.M., Chen, F.H., Hung, C.T., Ateshian, G.A., 2006. Frictional response of bovine articular cartilage under creep loading following proteoglycan digestion with chondroitinase ABC. J. Biomech. Eng. 128, 131–134.

Basalo, I.M., Mauck, R.L., Kelly, T.A., Nicoll, S.B., Chen, F.H., Hung, C.T., Ateshian, G.A., 2004. Cartilage interstitial fluid load support in unconfined compression following enzymatic digestion. J. Biomech. Eng. 126, 779–786.

Bonifasi-Lista, C., Lake, S.P., Small, M.S., Weiss, J.A., 2005. Viscoelastic properties of the human medial collateral ligament under longitudinal, transverse and shear loading. J. Orthop. Res. 23, 67–76.

Campbell, M.A., Tester, A.M., Handley, C.J., Checkley, G.J., Chow, G.L., Cant, A.E., Winter, A.D., Cain, W.E., 1996. Characterization of a large chondroitin sulfate proteoglycan present in bovine collateral ligament. Arch. Biochem. Biophys. 329, 181–190.

Chen, A.C., Bae, W.C., Schinagl, R.M., Sah, R.L., 2001. Depth- and strain-dependent mechanical and electromechanical properties of full-thickness bovine articular cartilage in confined compression. J. Biomech. 34, 1–12.

Cohen, B., Lai, W.M., Mow, V.C., 1998. A transversely isotropic biphasic model for unconfined compression of growth plate and chondroepiphysis. J. Biomech. Eng. 120, 491–496.

Cribb, A.M., Scott, J.E., 1995. Tendon response to tensile stress: an ultrastructural investigation of collagen:proteoglycan interactions in stressed tendon. J. Anat. 187, 423–428, Pt 2.

Danielson, K.G., Baribault, H., Holmes, D.F., Graham, H., Kadler, K.E., Iozzo, R.V., 1997. Targeted disruption of decorin leads to abnormal collagen fibril morphology and skin fragility. J. Cell Biol. 136, 729–743.

Elliott, D.M., Robinson, P.S., Gimbel, J.A., Sarver, J.J., Abboud, J.A., Iozzo, R.V., Soslowsky, L.J., 2003. Effect of altered matrix proteins on quasilinear viscoelastic properties in transgenic mouse tail tendons. Ann. Biomed. Eng. 31, 599–605.

Ernst, S., Langer, R., Cooney, C.L., Sasisekharan, R., 1995. Enzymatic degradation of glycosaminoglycans. Crit. Rev. Biochem. Mol. Biol. 30, 387–444.

Farndale, R.W., Buttle, D.J., Barrett, A.J., 1986. Improved quantitation and discrimination of sulphated glycosaminoglycans by use of dimethylmethylene blue. Biochim. Biophys. Acta 883, 173–177.

Federico, S., Herzog, W., 2008. On the anisotropy and inhomogeneity of permeability in articular cartilage. Biomech. Model Mechanobiol. 7, 367–378.

Fessel, G., Snedeker, J.G., 2009. Evidence against proteoglycan mediated collagen fibril load transmission and dynamic viscoelasticity in tendon. Matrix Biol. 28, 503–510.

Franchi, M., Raspanti, M., Dell'Orbo, C., Quaranta, M., De Pasquale, V., Ottani, V., Ruggeri, A., 2008. Different crimp patterns in collagen fibrils relate to the subfibrillar arrangement. Connect. Tissue Res. 49, 85–91.

Gardiner, J.C., Weiss, J.A., 2003. Subject-specific finite element analysis of the human medial collateral ligament during valgus knee loading. J. Orthop. Res. 21, 1098–1106.

Gillard, G.C., Merrilees, M.J., Bell-Booth, P.G., Reilly, H.C., Flint, M.H., 1977. The proteoglycan content and the axial periodicity of collagen in tendon. Biochem. J. 163, 145–151.

Gu, W.Y., Mao, X.G., Foster, R.J., Weidenbaum, M., Mow, V.C., Rawlins, B.A., 1999. The anisotropic hydraulic permeability of human lumbar anulus fibrosus. Influence of age, degeneration, direction, and water content. Spine 24, 2449–2455.

Han, S., Gemmell, S.J., Helmer, K.G., Grigg, P., Wellen, J.W., Hoffman, A.H., Sotak, C.H., 2000. Changes in ADC caused by tensile loading of rabbit achilles tendon: evidence for water transport. J. Magn. Reson. 144, 217–227.

Hascall, V.C., 1977. Interaction of cartilage proteoglycans with hyaluronic acid. J. Supramol. Struct. 7, 101–120.

Helmer, K.G., Wellen, J., Grigg, P., Sotak, C.H., 2004. Measurement of the spatial redistribution of water in rabbit Achilles tendon in response to static tensile loading. J. Biomech. Eng. 126, 651–656.

Henninger, H.B., Maas, S.A., Underwood, C.J., Whitaker, R.T., Weiss, J.A., 2007. Spatial distribution and orientation of dermatan sulfate in human medial collateral ligament. J. Struct. Biol. 158, 33–45.

Henninger, H.B., Maas, S.A., Shepherd, J.H., Joshi, S., Weiss, J.A., 2009. Transversely isotropic distribution of sulfated glycosaminoglycans in human medial collateral ligament: a quantitative analysis. J. Struct. Biol. 165, 176–183.

Hewitt, J., Guilak, F., Glisson, R., Vail, T.P., 2001. Regional material properties of the human hip joint capsule ligaments. J. Orthop. Res. 19, 359–364.

Holmes, M.H., 1986. Finite deformation of soft tissue: analysis of a mixture model in uni-axial compression. J. Biomech. Eng. 108, 372–381.

Holmes, M.H., Mow, V.C., 1990. The nonlinear characteristics of soft gels and hydrated connective tissues in ultrafiltration. J. Biomech. 23, 1145–1156.

Huang, C.Y., Stankiewicz, A., Ateshian, G.A., Mow, V.C., 2005. Anisotropy, inhomogeneity, and tension-compression nonlinearity of human glenohumeral cartilage in finite deformation. J. Biomech. 38, 799–809.

Ilic, M.Z., Carter, P., Tyndall, A., Dudhia, J., Handley, C.J., 2005. Proteoglycans and catabolic products of proteoglycans present in ligament. Biochem. J. 385, 381–388.

Iozzo, R.V., 1998. Matrix proteoglycans: from molecular design to cellular function. Annu. Rev. Biochem. 67, 609–652.

Iozzo, R.V., 1999. The biology of the small leucine-rich proteoglycans. Functional network of interactive proteins. J. Biol. Chem. 274, 18843–18846.

Katta, J., Stapleton, T., Ingham, E., Jin, Z.M., Fisher, J., 2008. The effect of glycosaminoglycan depletion on the friction and deformation of articular cartilage. Proc. Inst. Mech. Eng., Part H: J. Eng. Med. 222, 1–11.

Korhonen, R.K., Laasanen, M.S., Töyräs, J., Lappalainen, R., Helminen, H.J., Jurvelin, J.S., 2003. Fibril reinforced poroelastic model predicts specifically mechanical behavior of normal, proteoglycan depleted and collagen degraded articular cartilage. J. Biomech. 36, 1373–1379.

Korhonen, R.K., Laasanen, M.S., Toyras, J., Rieppo, J., Hirvonen, J., Helminen, H.J., Jurvelin, J.S., 2002. Comparison of the equilibrium response of articular cartilage in unconfined compression, confined compression and indentation. J. Biomech. 35, 903–909.

Li, G., Suggs, J., Gill, T., 2002. The effect of anterior cruciate ligament injury on knee joint function under a simulated muscle load: a three-dimensional computational simulation. Ann. Biomed. Eng. 30, 713–720.

Lujan, T.J., Underwood, C.J., Jacobs, N.T., Weiss, J.A., 2009. Contribution of glycosaminoglycans to viscoelastic tensile behavior of human ligament. J. Appl. Physiol. 106, 423–431.

Lujan, T.J., Underwood, C.J., Henninger, H.B., Thompson, B.M., Weiss, J.A., 2007. Effect of dermatan sulfate glycosaminoglycans on the quasi-static material properties of the human medial collateral ligament. J. Orthop. Res. 25, 894–903.

Lynch, H.A., Johannessen, W., Wu, J.P., Jawa, A., Elliott, D.M., 2003. Effect of fiber orientation and strain rate on the nonlinear uniaxial tensile material properties of tendon. J. Biomech. Eng. 125, 726–731.

Maroudas, A., Schneiderman, R., 1987. "Free" and "exchangeable" or "trapped" and "non-exchangeable" water in cartilage. J. Orthop. Res. 5, 133–138.

Provenzano, P.P., Vanderby Jr., R., 2006. Collagen fibril morphology and organization: implications for force transmission in ligament and tendon. Matrix Biol. 25, 71–84.

Quinn, T.M., Dierickx, P., Grodzinsky, A.J., 2001. Glycosaminoglycan network geometry may contribute to anisotropic hydraulic permeability in cartilage under compression. J. Biomech. 34, 1483–1490.

Redaelli, A., Vesentini, S., Soncini, M., Vena, P., Mantero, S., Montevecchi, F.M., 2003. Possible role of decorin glycosaminoglycans in fibril to fibril force transfer in relative mature tendons—a computational study from molecular to microstructural level. J. Biomech. 36, 1555–1569.

Reese, S.P., Maas, S.A., Weiss, J.A., 2010. Micromechanical models of helical superstructures in ligament and tendon fibers predict large Poisson's ratios. J. Biomech. 43, 1394–1400.

Rigozzi, S., Muller, R., Snedeker, J.G., 2009. Local strain measurement reveals a varied regional dependence of tensile tendon mechanics on glycosaminoglycan content. J. Biomech. 42, 1547–1552.

Robinson, P.S., Huang, T.F., Kazam, E., Iozzo, R.V., Birk, D.E., Soslowsky, L.J., 2005. Influence of decorin and biglycan on mechanical properties of multiple tendons in knockout mice. J. Biomech. Eng. 127, 181–185.

Sakane, M., Livesay, G.A., Fox, R.J., Rudy, T.W., Runco, T.J., Woo, S.L., 1999. Relative contribution of the ACL, MCL, and bony contact to the anterior stability of the knee. Knee Surg. Sports Traumatol. Arthrosc. 7, 93–97.

Scott, J.E., 2003. Elasticity in extracellular matrix 'shape modules' of tendon, cartilage, etc. a sliding proteoglycan-filament model. J. Physiol. 553, 335–343.

Screen, H.R., Shelton, J.C., Chhaya, V.H., Kayser, M.V., Bader, D.L., Lee, D.A., 2005. The influence of noncollagenous matrix components on the micromechanical environment of tendon fascicles. Ann. Biomed. Eng. 33, 1090–1099.

Seog, J., Dean, D., Rolauffs, B., Wu, T., Genzer, J., Plaas, A.H., Grodzinsky, A.J., Ortiz, C., 2005. Nanomechanics of opposing glycosaminoglycan macromolecules. J. Biomech. 38, 1789–1797.

Setton, L.A., Zhu, W., Mow, V.C., 1993. The biphasic poroviscoelastic behavior of articular cartilage: role of the surface zone in governing the compressive behavior. J. Biomech. 26, 581–592.

Soltz, M.A., Ateshian, G.A., 2000. Interstitial fluid pressurization during confined compression cyclical loading of articular cartilage. Ann. Biomed. Eng. 28, 150–159.

Swartz, M.A., Fleury, M.E., 2007. Interstitial flow and its effects in soft tissues. Annu. Rev. Biomed. Eng. 9, 229–256.

van Driel, W.D., van Leeuwen, E.J., Von den Hoff, J.W., Maltha, J.C., Kuijpers-Jagtman, A.M., 2000. Time-dependent mechanical behaviour of the periodontal ligament. Proc. Inst. Mech. Eng., Part H: J. Eng. Med. 214, 497–504.

Vogel, K.G., Ordog, A., Pogany, G., Olah, J., 1993. Proteoglycans in the compressed region of human tibialis posterior tendon and in ligaments. J. Orthop. Res. 11, 68–77.

Weiss, J.A., Maakestad, B.J., 2006. Permeability of human medial collateral ligament in compression transverse to the collagen fiber direction. J. Biomech. 39, 276–283.

Weiss, J.A., Gardiner, J.C., Bonifasi-Lista, C., 2002. Ligament material behavior is nonlinear, viscoelastic and rate-independent under shear loading. J. Biomech. 35, 943–950.

Wellen, J., Helmer, K.G., Grigg, P., Sotak, C.H., 2004. Application of porous-media theory to the investigation of water ADC changes in rabbit Achilles tendon caused by tensile loading. J. Magn. Reson. 170, 49–55.

Williamson, A.K., Chen, A.C., Sah, R.L., 2001. Compressive properties and function–composition relationships of developing bovine articular cartilage. J. Orthop. Res. 19, 1113–1121.

Yin, L., Elliott, D.M., 2004. A biphasic and transversely isotropic mechanical model for tendon: application to mouse tail fascicles in uniaxial tension. J. Biomech. 37, 907–916.